



MADRID
inter.noise 2019
June 16 - 19

NOISE CONTROL FOR A BETTER ENVIRONMENT

Identification of noise source for the model support in wind tunnel test section

Wang ,Shuai

**School of Marine Science and Technology, Northwestern Polytechnical University
Research & Development Institute of Northwestern Polytechnical University in
Shenzhen, Northwestern Polytechnical University
127 Youyi Road(West), Beilin, Xi'an City, Shanxi Province, PRC**

Liao ,Daxiong

**Chain Aerodynamics Research and Development Center, Mianyang City, Sichuan
Province, China**

Wang ,Minqing¹

**School of Marine Science and Technology, Northwestern Polytechnical University
Research & Development Institute of Northwestern Polytechnical University in
Shenzhen, Northwestern Polytechnical University
127 Youyi West Road, Beilin District, Xi'an City, Shaanxi Province, China**

Zhang ,Huadong

**School of Marine Science and Technology, Northwestern Polytechnical University
Research & Development Institute of Northwestern Polytechnical University in
Shenzhen, Northwestern Polytechnical University
127 Youyi West Road, Beilin District, Xi'an City, Shaanxi Province, China**

Lei ,Yu

**School of Marine Science and Technology, Northwestern Polytechnical University
Research & Development Institute of Northwestern Polytechnical University in
Shenzhen, Northwestern Polytechnical University
127 Youyi West Road, Beilin District, Xi'an City, Shaanxi Province, China**

ABSTRACT

When a model support is exploited for acoustic test in a wind tunnel, noise from the model support aerodynamic performance and the sound radiation due to the flow-induced model vibration can be found in the test section. Corresponding simulations and experiments are conducted for identifying the main noise source. The finite element model of aerodynamic model support is established, and the aerodynamic noise of 1.3Ma is obtained. Furthermore, sound radiation of the model support is calculated when the tested flow shock load is applied in a finite element software. Comparison among the aerodynamic noise, sound radiation and the experimental value demonstrates that the aerodynamic noise of the model support is much larger than the sound radiation, and the aerodynamic noise is comparative with the experimental value, which draws the conclusion that the aerodynamic noise is the main noise source in the test section of the wind tunnel.

¹ mqwang@nwpu.edu.cn

Investigation in this paper provides guidance for future noise reduction of the background.

Keywords: model support, aerodynamic noise, sound radiation

I-INCE Classification of Subject Number: 76

1. INTRODUCTION

As an indispensable part of the wind tunnel test section, the model support has its own specific noise characteristics. Noise caused by model support includes aerodynamic noise and sound radiated from vibration induced by flow. When the wind tunnel is in the operative mode, the mixture of the noise is generated, which leads to difficulty in the noise control of model support. Therefore, identifying the noise source of the model support is of great significance for future noise control of test section.

Currently, computational fluid dynamics(CFD) coupling acoustic analogy method is the main method for aerodynamic noise prediction , and has certain applicability . While finite element method (FEM) and boundary element method (BEM) are used to calculate and analyze the noise of high-speed pantograph [2]. Talotte [3] studied the noise calculation including aerodynamic noise calculation method optimization under the condition of high velocity, and proposed a more advantageous aerodynamic noise calculation method. Umesh and Paliath [4] studied the influence of mechanical equipment installation location on aerodynamic noise using the high-order finite difference large eddy model coupling FW-H (Ffowcs Williams & Hawkings) equation. Since Blevins [5] proposed the concept of flow induced vibration, Matthias Springer [6] and Schafer [7] investigated the sound radiation caused by the interaction between acoustic medium and flexible structure thoroughly. Everstine [8] summarized various finite element calculation methods to solve the interaction problems between acoustics, fluid and structures. Lara [9], Qu [10] and Schmidt [11] respectively simulated and analyzed sound radiation under different structures and conditions, thus concluded sound radiation characteristics under different conditions.

With rapid development of the aerodynamic noise calculation method, the analysis accuracy and applicability are improved unceasingly. Various research methods on sound radiation have complementary advantages in sound radiation analysis under acoustic, fluid-solid coupling fields, which provide a basis for radiation noise control and structural optimization. The existing studies mainly focus on the optimization of aerodynamic noise calculation method and the analysis of sound radiated from vibration. However, there are few references on the noise characteristics of wind tunnel model supports, and few scholars notice the noise of wind tunnel test section from the perspective of model supports.

The purpose of this study is to identify the noise source of the test section model support and provide a basis for effectively reducing the background noise of the test section in the future. The aerodynamic noise finite element model and the sound radiation finite element model of the model support are established respectively, and the aerodynamic noise and the sound radiated from vibration of the model support were obtained. The aerodynamic noise and sound radiation of the model support are sorted, by comparing the simulation results.

2. Theoretical analysis of aerodynamic noise and sound radiation

2.1 Numerical calculation method of aerodynamic noise

Separating flow field calculation and acoustic field calculation from each other is one of the characteristics in mixed calculation method of acoustic analogy. In this paper, the FW-H equation of aerodynamic noise is used to calculate the aerodynamic noise of the model support. Which is based on obtaining the flow solution of the model support near the field, taken the flow field information as the acoustic source signal, using the FW-H equation to obtain the aerodynamic noise value at the monitoring point. FW-H equation can be written as

$$\begin{aligned} \left(\frac{1}{c^2} \frac{\partial^2}{\partial t^2} - \frac{\partial^2}{\partial x_i^2}\right) \rho'(x, t) = \frac{\partial}{\partial t} \{[\rho_0 v_n + \rho(u_n - v_n)]\delta(f)\} \\ - \frac{\partial}{\partial x_i} \{[-P'_{i,j} n_j + \rho u_i(u_n - v_n)]\delta(f)\} + \frac{\partial^2}{\partial x_i \partial x_j} [(T_{i,j} H(f))] \end{aligned} \quad (1)$$

where, u_n , v_n are the normal velocity of the control surface and the normal velocity of the fluid; u_i is the velocity component of the fluid in the x_i direction; $H(f)$ is Heaviside function; $\delta(f)$ is the Dirac delta function; P_{ij} and T_{ij} are the stress tensor and Lighthill tensor respectively. The three terms at the right end of Equation (1) are thickness noise source, load noise source and quadrupole noise source respectively.

By using FW-H-pds method [12], the integral surface of FW-H equation is reinterpreted as the penetrable integral surface, and the solution of FW-H equation can be obtained

$$P'(x, t) = P'_M(x, t) + P'_D(x, t) + P'_O(x, t) \quad (2)$$

$$P'_M(x, t) = \frac{1}{4\pi} \iint_s \left[\frac{\rho_0 (\dot{U}_n + U_{\dot{n}})}{r(1-M_r)^2} \right]_{ret} dS + \frac{1}{4\pi} \iint_s \left[\frac{\rho_0 U_n (r\dot{M}_r + c_0 M_r - c_0 M^2)}{r^2(1-M_r)^3} \right]_{ret} dS \quad (3)$$

$$P'_D(x, t) = \frac{1}{4\pi c_0} \iint_s \left[\frac{\dot{L}_r}{r(1-M_r)^2} \right]_{ret} dS + \frac{1}{4\pi} \iint_s \left[\frac{L_r - L_M}{r^2(1-M_r)^2} \right]_{ret} dS \quad (4)$$

$$\begin{aligned} + \frac{1}{4\pi c_0} \iint_s \left[\frac{L_r (r\dot{M}_r + c_0 M_r - c_0 M^2)}{r^2(1-M_r)^3} \right]_{ret} dS \\ \begin{cases} U_i = (1 - \rho / \rho_0) v_i + \rho u_i / \rho_0 \\ L_i = -P'_{i,j} n_j + \rho u_i (u_n - v_n) \end{cases} \end{aligned} \quad (5)$$

where, P' , P'_M , P'_D and P'_O are the total sound pressure, thickness noise sound pressure, load noise sound pressure and four-level sub-sound pressure, respectively; f , x and t are the integral plane, observer position and receiving time, respectively; ρ and c are density and sound velocity; M , s , u , v are Mach number, area, disturbance velocity and motion velocity respectively; “.” is the derivative with respect to time; The subscript “ret” is the delay time; The subscripts “i” and “j” are the projections in the i and j directions.

The acoustic integral surface used in the integral formula can be any spatial surface containing solids. If the selected sound source integral surface is far away from the object surface, the calculated result can be considered as the total noise containing quadrupole noise. When the integrated surface of the sound source is selected as the surface of the object, the sound pressure obtained is linear, which includes the thickness noise and the load noise. The solution equation of aerodynamic noise is given by Equation (1). Combined with FW-H-pds method, a layer of grid surface of the model support is selected as the integral surface of the sound source, the aerodynamic noise of

the model support can be solved after the integration of the selected sound source integral surface.

2.2 Numerical calculation method of sound radiation

The fluid structure was established outside the model support structure, and the finite element mesh between the structure and the fluid was discretized for finite element analysis. When the acoustic medium vibrates slightly under external excitation, the sound pressure in the air outside the support structure can be expressed by using the Helmholtz equation

$$\nabla^2 + k_0^2 p = 0 \quad (6)$$

where, $k_0 = \omega / c$ is the sound wave number; ω is the circular frequency of the external excitation; c is the sound velocity in the fluid; p is the fluid pressure. Introducing operators of divergence and gradient in the form of vector, combined with the acoustic wave equation, the element matrix is obtained by discretizing Equation (6) with Galerkin method. At the same time, multiplied by the virtual variable δp of sound pressure, and integrated in the flow field area, the following can be obtained after calculation

$$\iiint_v \frac{1}{c^2} \delta p \frac{\partial^2 p}{\partial t^2} dV + \iiint_v (\{\mathbf{L}\}^T \delta p) (\{\mathbf{L}\} p) dV = \iint_{s+\Sigma} \{\mathbf{n}\}^T \delta p (\{\mathbf{L}\} p) dS \quad (7)$$

where $\{\mathbf{n}\}$ is the normal vector of the boundary surface S and Σ . Relation between the normal sound pressure gradient of the fluid and the normal acceleration of the structure is as follows

$$\{\mathbf{n}\} \cdot \{\nabla \pi\} = -\rho_f \{\mathbf{n}\} \cdot \frac{\partial^2 \{\mathbf{U}\}}{\partial t^2} \quad (8)$$

where, ρ_f is the density of the fluid medium; $\{\mathbf{U}\}$ is the displacement vector of the structure at the fluid-solid coupling surface. Its matrix form is

$$\{\mathbf{n}\}^T (\{\mathbf{L}\} p) = -\rho_f \{\mathbf{n}\}^T \left(\frac{\partial^2 \{\mathbf{U}\}}{\partial t^2} \right) \quad (9)$$

Substituting Equation (9) into Equation (7), discretizing the structure and fluid into several finite elements, the sound pressure at any point within fluid and the displacement of fluid-solid interface can be expressed by the node difference of the corresponding element. The finite element matrix is as follows

$$[\mathbf{M}_e^p] \{\ddot{\mathbf{p}}_e\} + [\mathbf{K}_e^p] \{\mathbf{p}_e\} + \rho_f [\mathbf{R}_e] \{\ddot{\mathbf{U}}_e\} = \{0\} \quad (10)$$

where, $[\mathbf{M}_e^p]$ is the fluid mass matrix; $[\mathbf{K}_e^p]$ is the fluid stiffness matrix; $\rho_f [\mathbf{R}_e]^T$ is the coupling mass matrix on the fluid-solid coupling surface. The elastic model support is located in the acoustic medium. Therefore, there is an interaction at the contact surface of the fluid and the model support. At present, the coupled vibration equation between the model support as an elastomer and the sound field is

$$[\mathbf{M}_e] \{\ddot{\mathbf{U}}_e\} + [\mathbf{K}_e] \{\mathbf{U}_e\} = \{\mathbf{F}_e\} + \{\mathbf{F}_f\} \quad (11)$$

where, $\{\mathbf{F}_f\}$ is the force exerted by the structure on the fluid. Combination of Equation (10) and (11), the finite element equations of the coupled system are derived

$$\begin{bmatrix} [\mathbf{M}_e] & 0 \\ \rho_f [\mathbf{R}_e]^T & [\mathbf{M}_e^p] \end{bmatrix} \begin{Bmatrix} \{\ddot{\mathbf{U}}_e\} \\ \{\ddot{\mathbf{P}}_e\} \end{Bmatrix} + \begin{bmatrix} [\mathbf{K}_e] & -\mathbf{R}^T \\ 0 & [\mathbf{K}_e^p] \end{bmatrix} \begin{Bmatrix} \{\mathbf{U}_e\} \\ \{\mathbf{P}_e\} \end{Bmatrix} = \begin{Bmatrix} \{\mathbf{F}_e\} \\ \{\mathbf{0}\} \end{Bmatrix} \quad (12)$$

When the fluid boundary is a fully absorbed boundary, the structural vibration characteristics and the sound pressure distribution in the flow field can be obtained by solving Equation (12), and then the sound radiation value caused by model support vibration in the fluid-solid coupling field can be obtained.

3. Model support noise calculation

3.1 Model validation

In order to verify the accuracy of the numerical finite element model of the physical model support. The finite element simulation calculation and test are carried out independently, and the data obtained by the two methods are compared and analyzed.

The physical model support is made of steel, and composed of multiple lamellar structures. So it is a typical thin-walled shell structure. When excited by the external load of fluid, the model support vibrates and radiates energy to surroundings, which constitutes the acoustic-induced coupling field between the model support and the test section. The first four natural frequencies of the model support are obtained the finite element model.

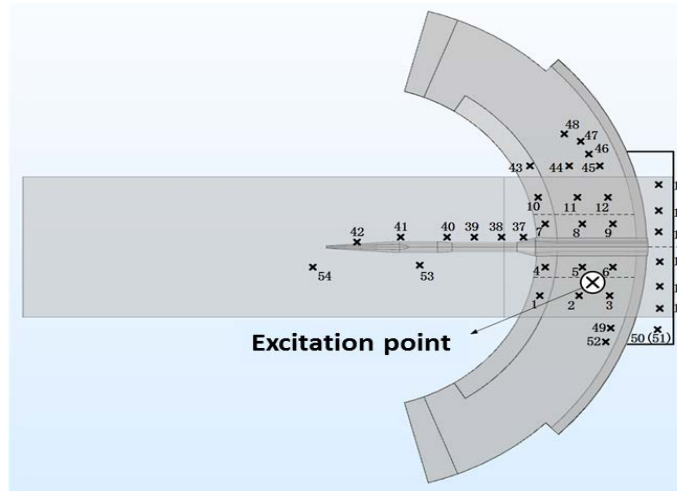


Figure 1: The diagram of support system excitation point and monitoring point position

During the modal characteristic test of the model support, the exciter is used to stimulate the model support, and the vibration acceleration of each measuring point is obtained. The position of excitation points and measure points are shown in Figure 1. The vibration response data of the three representative measuring points 6, 11 and 47 were selected, and the analysis showed that peak frequencies of 26Hz, 76Hz, 186Hz and 300Hz appeared in the spectrum curves of the three measuring points. Generally, these peak frequencies can be regarded as the modal frequencies of the structure. Table 1 shows the modal frequency results of test and finite element simulation.

Table 1: Modal frequency comparison between test and finite element simulation

type	1 st -order frequency	2 nd -order frequency	3 rd -order frequency	4 th -order frequency
test	26.5Hz	76.9Hz	186.2Hz	300.0Hz
simulation	26.6Hz	79.2Hz	162.3Hz	306.6Hz

It can be seen that the simulative modal frequencies have a little difference with those of the test result in Table 1. Moreover, the first, second and fourth modal frequencies are in good agreement, and the bending vibration modal frequencies of the two are nearly the same. The reason is that the actual model in the test is relatively complex, the ideal simplified model in the finite element simulation cannot completely approximate the actual structure. Therefore, it is feasible and effective to get the vibration characteristics of the model support through the finite element simulation method.

3.2 Numerical calculation of aerodynamic noise

Figure 2 shows the geometric model of the physical model support in the test section, including model support and square column. The model support is composed of a 10° half angle cone and a machete scaffold. The square column with section size of 0.6m×0.6m and length of 2.8m is set as solid wall boundary to simulate the wind tunnel test section. The upper and lower ends of the machete scaffold extend to the outside of the test section.

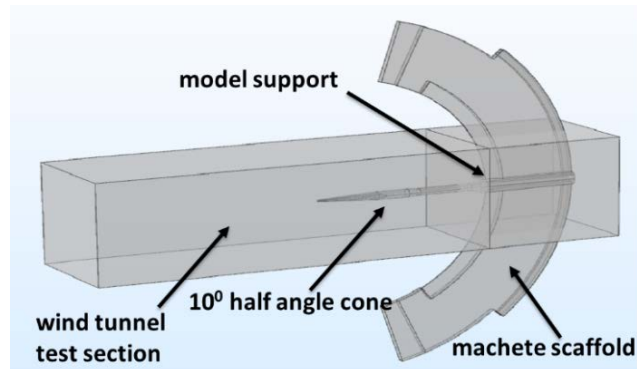


Figure 2: The finite element model of the model support system located in the test section

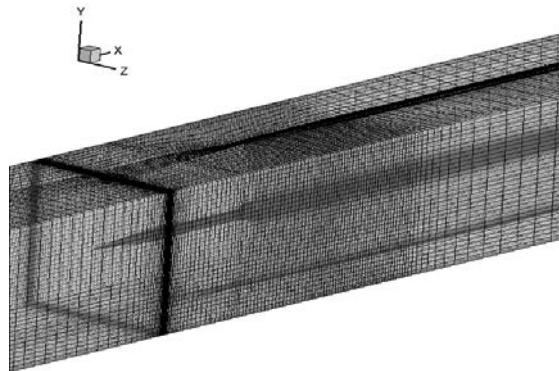


Figure 3: Finite element mesh of test section

Figure 3 shows the finite element mesh of test section, and the model grid is a structured multi-block grid. For the geometric characteristics of the model support, O-grid technology is used to generate the boundary layer grid, which is extended along the outward normal direction in a certain proportion to realize the mesh encryption on the surface of the model support. The total number of computational model grids is about 10 million. The upper and lower ends of the model support are outside the solid wall boundary of the test section, not affecting the calculation of the flow field in the test section, which is omitted in the calculation grid.

The numerical calculation model in this paper includes three kinds of boundaries which are test section inlet, test section outlet and object surface. The pressure inlet, pressure outlet and non-slip solid boundary wall conditions are used respectively. Figure 4 is a schematic diagram of the position of the simulation monitoring point. The position of the simulation monitoring point is consistent with that of the test measuring point.

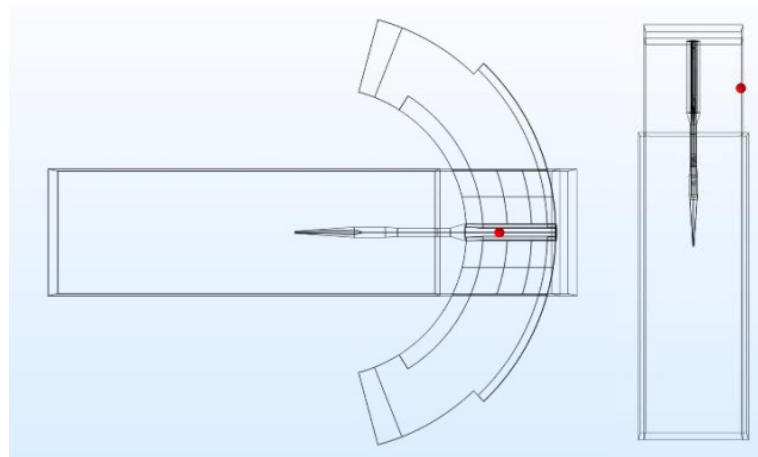


Figure 4: The diagram of monitoring point position

3.3 Numerical calculation of sound radiated from vibration

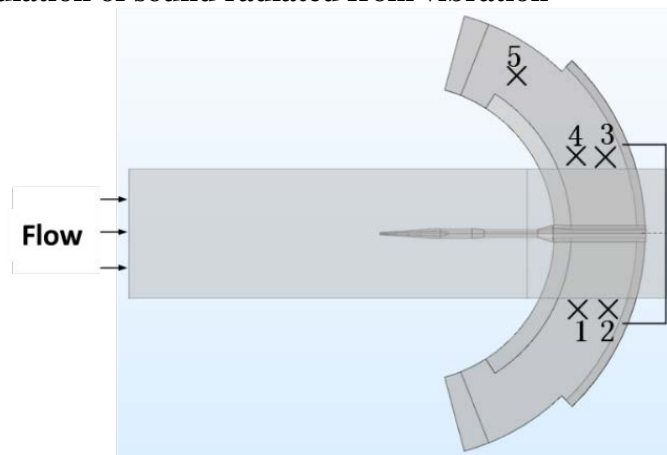


Figure 5: The diagram of sensor measuring point position of test section support system

The data of structural acceleration under flow are taken as the load data of the sound radiation of model support, which is calculated by using the finite element method of sound radiation in the coupling field.

Due to the high test velocity in the test section, the vibration sensor cannot be

arranged in the test section. Therefore, the sensor 1 to 5 measuring points were arranged in 5 positions of the model support structure as shown in Figure 5. Under the condition of 1.3Ma flow velocity, the vibration acceleration measured at each point was taken as the input load data of vibration sound radiation simulation. The input position of the load was the same as that of the sensor's measuring point. The position of the simulation monitoring point is shown in Figure 4.

The finite element grid of the coupling field in the test section of the model support is shown in Figure 6. The acoustic medium in the external field of the support is air. The model grid is a tetrahedral grid composed of 180815 domain units, 23960 boundary units and 3044 edge units.

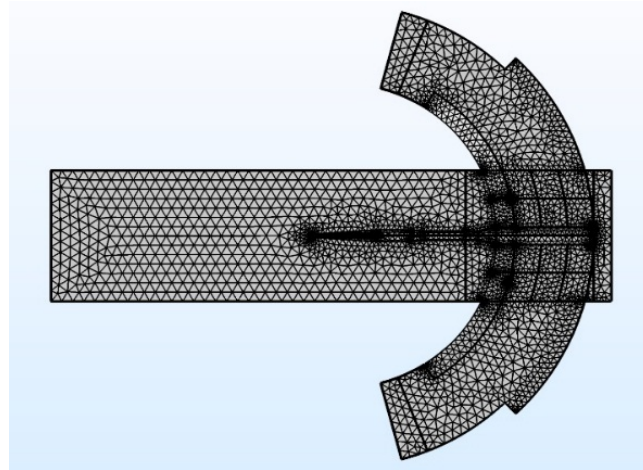


Figure 6: Finite element mesh of test section with model support system

4. Identification of noise source

Under the condition of 1.3Ma flow velocity, noise test was carried out in the section. The noise measurement point is located at the cave wall of the section where the model support located, as shown in Figure 4. The sensor used for noise measurement is the pressure field microphone with the range of 0~160dB and the accuracy of 0.1db. In order to reduce the noise generated by the microphone itself, the microphone was embedded into the cave wall in the experiment, and the cave wall of the test section was kept as smooth as possible.

With Fast Fourier Transform (FFT) applied to the pulsating pressure data measured in the wind tunnel, the noise value of the test point is obtained. Aerodynamic noise simulation, sound radiation simulation of flow-induced vibration, sound pressure level (as shown in Figure 7) and total sound pressure level (as shown in Figure 8) of test points have been compared.

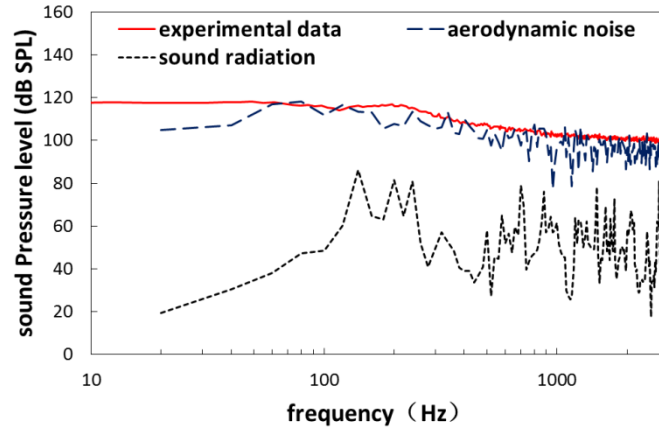


Figure 7: Comparison between the simulated value and the test value of sound pressure level

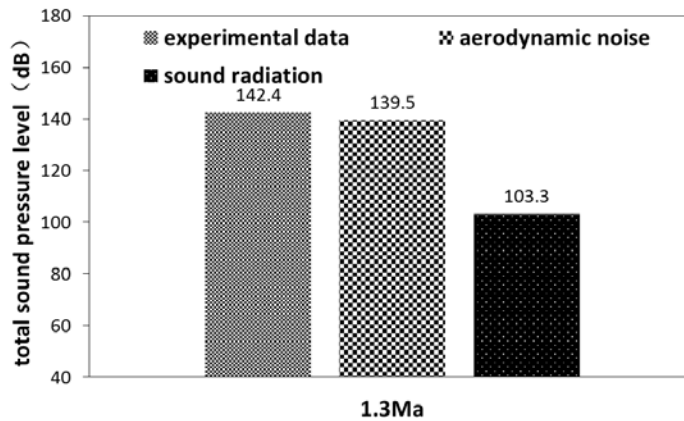


Figure 8: Comparison between the simulated value and the test value of total sound pressure level

As shown in Figure 7, the spectrum of aerodynamic noise is similar to that of test noise, while the spectrum of vibration noise radiated by model support structure is quite different from the other two, since the most important composition is omitted. As shown in Figure 8, the total sound pressure level of the model support structure under the condition of 1.3Ma flow velocity is 103.3dB, and the total sound pressure level obtained by the test is 142.4dB. The total sound pressure level of pneumatic noise is 139.5dB, slightly lower than the total sound pressure level obtained in the test. Therefore, it is found that one of the main noise sources in the section is the aerodynamic noise of the model support, while the sound radiated from vibration noise of the model support structure contributes less to the noise in the test section.

5. CONCLUSIONS

Based on the calculation of the aerodynamic noise and the sound radiation, comparing with the measured sound in the wind tunnel test section, the two main noise sources of model support is analysed in this paper. The main conclusions are as follows:

(1) In the frequency range of 20Hz-3kHz, the total sound pressure level of the aerodynamic noise of the model support is slightly lower than that of the test section, and their spectrum curves were basically the same. Therefore it is found that the aerodynamic noise of the model support contributes much more to the background noise

of the test section than the sound radiation.

(2) Based on the noise characteristics of model supports, more attention should be paid to the aerodynamic noise caused by model supports in the future noise control of wind tunnel test section. Therefore, it is an effective way of controlling the aerodynamic noise of the model support to reduce the noise in wind tunnel test section.

6. REFERENCES

- [1]. Chow E, Walter J, Arnette S, Yen J. “*Recent advances in large-scale aeroacoustic wind tunnels*”, AIAA (2002).
- [2]. Lei S, Chengchun,Z, Jing W, Luquan R . “Numerical analysis of aerodynamic noise of a high-speed pantograph”, International conference on digital manufacturing & automation (2013).
- [3]. Talotte C, Gautier P E, Thompson D J. “*Identification, modeling and reduction potential of railway noise sources: a critical survey*”, Journal of Sound & Vibration 267.3(2003):447-468.
- [4]. Umesh P, Sachin P. “*Large Eddy Simulation for Jet Installation Effects*”, AIAA 19th Aeroacoustics conference (2013).
- [5]. Blevins R. “*Flow-induced Vibration*”, New York: Van Nostrand Reinhold (1998).
- [6]. Matthias S, Christo P, Stefan B. “*Fluid-structure-acoustic coupling for a flat plate*”, International Journal of Heat and Fluid Flow 66(2017):249-257.
- [7]. Schäfer, Müller, Uffinger, Becker, Grabinger, “*Fluid-structure-acoustics interaction of the flow past a thin flexible structure*”, AIAA 48.4(2010):738-748.
- [8]. G.C. Everstine. “*Finite element formulations of structural acoustics problems*”, Computers and Structures 65.3(1997):307-321.
- [9]. Clara H, Sauer R. “*Simulation analysis of structural vibration sound radiation of oil and gas pipeline*”, Oil & Gas Storage & Transportation 2.1 (2012):193-225(33).
- [10]. Y Qu , J Su, H Hua, G Meng. “*Structural vibration and acoustic radiation of coupled propeller-shafting and submarine hull system due to propeller forces*”, Journal of Sound & Vibration 401(2017):76-93.
- [11]. PL Schmidt ,KD Frampton. “*Acoustic radiation from a simple structure in supersonic flow*”, Journal of Sound & Vibration 328.3(2009):243-258.
- [12]. Di Francescantonio P. “*A new boundary integral formulation for the prediction of sound radiation*”, Journal of Sound & Vibration 202.4 (1997) :491-509.